

relative humidity in the region of BrPn is only about 45% (ref. 3). Interestingly, it may eventually be possible to correct for the deuterium enrichment due to transpiration by analysing both hydrogen and oxygen isotope ratios in cellulose (see ref. 10).

A second source of scatter may arise from the fact that the surface temperatures used for comparison with the tree δD values are unweighted average annual temperatures. If the trees are incorporating annual precipitation, the δD value of this precipitation will probably be a weighted average of varying proportions of the various seasonal precipitations. Consequently, the unweighted temperature and weighted δD values may not always be uniformly related. Furthermore, the compared temperatures are those of meteorological stations which are not located at the exact site of tree growth. Thus, the pattern of geographical temperature variation of these stations may not be exactly analogous to that of the growth sites.

Biochemical or physiological differences between these 20 different 'well-behaved' trees could produce some, as yet, unrecognized differences in the net hydrogen isotope fractionation between leaf water and cellulose C-H hydrogen. Such differences might contribute to the scatter in Fig. 3.

There may also be trees among the 20 'well-behaved' samples that have not incorporated average annual precipitation. Instead, some trees may have utilized relatively more water from a single season. When plotted against annual temperature, the δD values of these trees might produce some scatter such as appears in Fig. 3.

Finally, there is likely to be scatter in the primary precipitation δD /temperature relationship (see Fig. 2). This scatter would be manifested in Fig. 3, if the δD values of the trees reflected the δD values of the local meteoric waters.

In spite of these possible sources of scatter in the relationship between tree δD values and annual temperature, Fig. 3 shows that such a relationship does exist. Furthermore, for the 20 'well-behaved' samples of Fig. 3, the relationship is quite close to that which might be expected if the δD variations of the trees mimic those of the local annual precipitation.

Thus, trees from the proper sites seem to record δD values that correspond to geographical climatic differences. Note that

the samples analysed for this work were collected by individuals who had little specific instruction regarding the relative merits of local tree sites. Thus, local site selection was largely random. From information supplied by individuals who collected the samples (see ref. 3), it seems that the 'well-behaved' sites are likely to be those in which there is an absence of stagnant soil, ground or surface water¹⁹

Conclusion

A comparison of the geographical variation of the δD values of trees with the associated average annual temperature reveals an overall correlation for many sites and species of trees. The spatial linear temperature coefficient obtained for δD values from 20 widely separated tree samples in North America is $5.8\% \text{ } ^\circ\text{C}^{-1}$. This compares with a temperature coefficient of $5.6\% \text{ } ^\circ\text{C}^{-1}$ obtained from annual precipitation δD values at 11 North American IAEA sites. The similarity of these two coefficients is consistent with the idea that the δD variations of the trees reflect the δD variations of the local precipitation. The latter conclusion is supported by the spatial distribution of the tree δD values (Fig. 1). These δD values decrease from the coast to the interior and from south to north. This pattern of variation is analogous to that observed for meteoric waters over North America (Fig. 1).

Site conditions seem to be important in determining the δD values recorded by trees, and some site conditions can produce scatter in plots of annual temperatures against tree δD values on a spatial scale. However, the trees sampled for this work indicate that favourable growth sites are common.

The geographical temperature-tree δD correlation for seven widely separated North American trees shows a remarkable consistency over the interval 1931-70. This consistency is maintained in spite of the differences in both species and relative ages of the seven tree samples involved.

We thank everyone who provided samples for this work (see ref. 3 for names). NSF grant ATM80-18830 supported this research. This is contribution no. 3691 of the Division of Geological and Planetary Sciences, California Institute of Technology.

Received 31 December 1981; accepted 18 March 1982.

1. Epstein, S., Yapp, C. J. & Hall, J. H. *Earth planet. Sci. Lett.* **30**, 241 (1976).
2. DeNiro, M. J. & Epstein, S. *Science* **204**, 51 (1979).
3. Yapp, C. J. & Epstein, S. *Geochim cosmochim Acta* (submitted).
4. Dansgaard, W. *Tellus* **16**, 436 (1964).
5. Friedman, I., Redfield, A. C., Schoen, B. & Harris, J. *Rev. Geophys.* **2**, 177 (1964).
6. Siegenthaler, U. & Oeschger, H. *Nature* **285**, 314 (1980).
7. Craig, H. *Science* **133**, 1833 (1961).
8. Gray, J. & Thompson, P. *Nature* **262**, 481 (1976).
9. Burk, R. L. & Stuiver, M. *Science* **211**, 1417 (1981).

10. Epstein, S., Thompson, P. & Yapp, C. J. *Science* **198**, 1209 (1977).
11. Schiegl, W. E. *Nature* **251**, 582 (1974).
12. Libby, L. M. & Pandolfi, L. J. *Proc. natn. Acad. Sci. U.S.A.* **71**, 2482 (1974).
13. Wilson, A. T. & Grinstead, M. J. *Nature* **257**, 387 (1975).
14. Epstein, S. & Yapp, C. J. *Earth planet. Sci. Lett.* **30**, 252 (1976).
15. Epstein, S. & Yapp, C. J. *Nature* **266**, 477 (1977).
16. Epstein, S. *Earth planet. Sci. Lett.* **39**, 303 (1978).
17. DeNiro, M. J. *Earth planet. Sci. Lett.* **54**, 177 (1981).
18. *Technical Report Series* Nos. 96, 117, 147 (IAEA, Vienna 1969, 1970, 1973).
19. Yapp, C. J. thesis, California Inst. Technol. (1980).

β Decay and the origins of biological chirality: experimental results

D. W. Gidley, A. Rich & J. Van House

Physics Department, University of Michigan, Ann Arbor, Michigan 48109, USA

P. W. Zitzewitz

Department of Natural Sciences, University of Michigan-Dearborn, Dearborn, Michigan, 48128, USA

A spin-polarized low-energy positron beam has been used to set limits on asymmetric positronium formation in optically active molecules. No asymmetry was found at the 7×10^{-4} level in cystine and tryptophan, but a possible effect of $(31 \pm 7) \times 10^{-4}$ was found in leucine. A quantitative connection is made with the origin of biological optical activity.

THE amino acids and sugars on which terrestrial life is based show maximal optical activity, that is, with rare exceptions, they are composed of D-sugars in RNA and DNA and L-amino acids in proteins. This observation poses the questions: (1) Why should life be based on optically active substances? (2) Are there any causal mechanisms that would lead us to expect the selection of the L-amino acids in terrestrial organisms and is

this choice expected to be the one statistically preferred when all possible biospheres are considered? Question (1) has been discussed extensively^{1,2} and there is widespread agreement that life should naturally select an ordered system based on optically pure substances. However, question (2), still unanswered, is one of the important problems in chemical and biological evolution.

In the absence of any causal mechanisms, the presently observed complete optical purity would be the result of a random fluctuation in the presumed virtually racemic isomeric balance of the primordial Earth, followed by chemical and biological amplification. The probability of selecting a particular isomer would then be 50%. On the other hand, causal mechanisms can systematically produce an isomeric excess which, if large enough to compete with random fluctuations, may strongly bias the odds on which isomer will eventually dominate. To generalize our treatment of question (2) to all types of biospheres it is necessary to distinguish two types of causal mechanisms: local and universal. A local causal mechanism relies on some local asymmetry to produce a bias in the odds on which isomer dominates in that particular biosystem. By contrast, a universal causal mechanism produces a systematic bias in the odds in favour of one isomer dominating throughout all biosystems in which it is effective. All such mechanisms must be related to the weak interaction as this is the only interaction that universally violates parity conservation. No reproducible quantitative results are yet available for either the random or causal mechanisms. The description, theoretical analysis, and preliminary experimental results of a new method to investigate the most plausible universal causal mechanism, preferential radiolysis by electrons emitted in the β decay of radionuclides, is the subject of this and the accompanying article³. For completeness, we also present a brief discussion of the leading local causal mechanism, preferential photolysis or catalysis by circularly polarized sunlight.

Analysis of two causal mechanisms

Preferential photolysis by circularly polarized light: Asymmetric effects have been observed in the interaction between amino acid isomers and circularly polarized light⁴. In addition, a circular polarization (CP) of sunlight of 0.1% has been observed at dawn and dusk in an IR band (780–800 nm)⁵. However, a corresponding CP in the UV, needed for asymmetric photolysis, was not found, and thus it must be <0.01%. In addition, because CP is a result of parity conserving electromagnetic interactions in the atmosphere, it can only be a local causal mechanism, that is, it must be identically zero when averaged over one Earth rotation and over the Earth's surface, unless non-uniformities exist in time (morning compared with

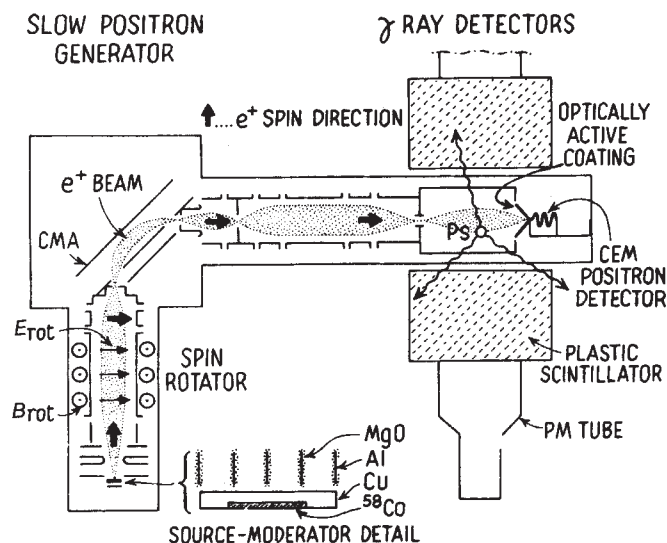


Fig. 1 The experimental apparatus used to measure asymmetries in triplet positronium formation. The beam consists of 3×10^3 positrons s^{-1} and initial helicity $h_0(e^+) = 0.21 \pm 0.02$ (ref. 13). The Wien filter spin rotator (crossed electric and magnetic fields) allows rotation of the average spin direction ($\langle \hat{s}_i \rangle$) of the beam with minimal effect on the average direction of the beam's momentum ($\langle \hat{p}_i \rangle$). Thus $h_0(e^+)$ may be continuously varied from $+0.21$ to -0.21 .

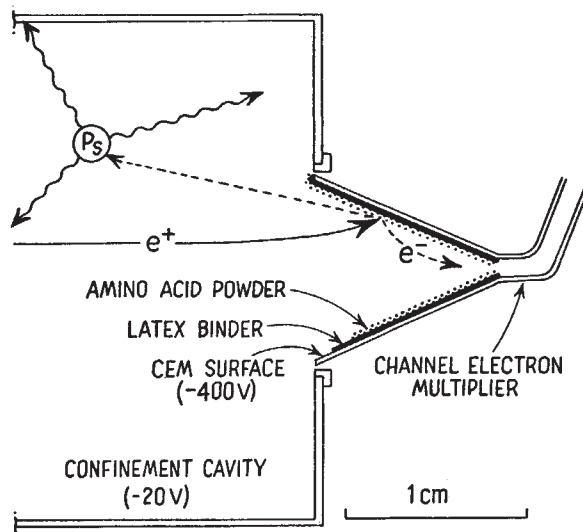


Fig. 2 Detail of the slow positron target region. A 0.5-mm thick layer of powder of a given sample was pressed on a binding layer of latex on the CEM cone. Measurements of Ps formation on the bare cone, the latex binder, and the amino acids confirmed that Ps formation occurred only in the amino acid layer. Secondary electrons are collected into the channel of the CEM. The triplet Ps formed in the amino acid powder lives a sufficient time to escape from the powder into the confinement cavity and annihilate into three γ rays with approximately the vacuum lifetime of 140 ns.

evening) and with respect to the Northern and Southern Hemispheres.

Preferential radiolysis related to electron helicity in β decay: The radiolysing β decay electrons, on emission from the nucleus, possess a handedness or helicity (h), that is—there is a correlation between the direction of the spin angular momentum and the linear momentum. This correlation is expressed by the relation $h = \langle h_i \rangle = \langle \hat{s}_i \cdot \hat{p}_i \rangle$ where, for the i th particle, \hat{s}_i is the Pauli spin matrix, \hat{p}_i the unit momentum vector ($\hat{p}_i = \hat{p}_i / |\hat{p}_i|$), h_i is the helicity operator, and the angular brackets represent an average over all particles in the ensemble. Further, for the present discussion $\langle \hat{s}_i \cdot \hat{p}_i \rangle = \langle \hat{s}_i \rangle \cdot \langle \hat{p}_i \rangle$, that is the positron spin and momenta are decoupled. If, for example, all spins and all momenta in a beam are parallel ($\langle \hat{s}_i \rangle = 1$ and $\langle \hat{p}_i \rangle = 1$). Preferential radiolysis by β decay electrons represents what we have defined as a universal causal mechanism and the problem is to determine to what degree this handed radiation could asymmetrically radiolyse racemic mixtures of amino acids on the primordial Earth.

Many experiments have searched for helicity induced preferential radiolysis⁶⁻⁸ but no reproducible effect has been demonstrated. We feel that this is because none of the experiments approached the level of sensitivity necessary to observe the small asymmetric effects which are now predicted to occur³. These effects arise from the distortion in the electronic wavefunctions in optically active molecules. The distortion induced by coupling between spin and orbital motion in the bound electrons produces a helicity per unit volume or helicity density—denoted $h(\vec{r})$. From considerations of parity conservation (mirror symmetry) $h(\vec{r})$ is zero for symmetric spin-unpolarized molecules but $h(\vec{r})$ can be non-zero for spin-unpolarized dissymmetric molecules.

The spin-dependent exchange interaction between the molecular electrons and the incident β decay electrons, when the coupling between $h(e^-)$, the helicity of the incident electrons, and $h(\vec{r})$ is included, produces an asymmetry, A_R , in the respective rates of radiolysis of L and D isomers $R(L)$, $R(D)$. On either reversal of $h(e^-)$ ($h(e^-) \rightarrow -h(e^-)$) or interchange of the L and D isomers this asymmetry may be written as:

$$A_R \equiv \frac{R^+(L) - R^-(L)}{R^+(L) + R^-(L)} = \frac{R^+(L) - R^+(D)}{R^+(L) + R^+(D)} \\ = |h(e^-)| H_R(E, Z) \quad (1)$$

Here (+, -) refers to $h(e^-) > 0$ or $h(e^-) < 0$ and from parity conservation $R^{\pm(D)} = R^{\mp(L)}$ so that, for example, A_R may be written as:

$$A_R = [R^-(D) - R^+(D)] / [R^-(D) + R^+(D)]$$

H_R , an effect of the molecular helicity density $h(\vec{r})$, is essentially an average of $h(\vec{r})$ weighted by the Coulomb interaction between the projectile (β) electron and the target (molecular) electrons. For projectile energies E_p of the order of 100–500 keV, H_R is given by the relation

$$H_R = \eta'_R (\alpha Z)^2 \frac{1}{2E_p \ln(2E_p)}$$

where α is the fine structure constant ($\alpha^{-1} \sim 137$), Z the atomic number of the heaviest atom in the asymmetric environment of the molecule and η'_R is a molecular asymmetry factor which takes into account the effect of molecular structure on H_R . See the accompanying article for a complete discussion of H_R . We note here that at $E_p \sim 100$ keV and $Z = 6$, H_R lies in the range $10^{-11} < H_R < 10^{-10}$. The uncertainty in H_R is primarily a result of the uncertainties of the molecular wave functions used in its calculation. Thus even if we take $h(e^-) = 1$ and assume that it does not decrease as the β slows down, (in fact $h(e^-) \rightarrow 0$ as the β slows down due to velocity dispersion caused by scattering⁹), the largest resulting value of A_R ($A_R < 10^{-10}$) would still be much too small to be observed in a direct radiolysis experiment. Current techniques limit such experiments to detection of $A_R > 10^{-3}$.

Larger effects, though less directly related to $h(\vec{r})$, may in fact be obtained by performing scattering experiments using unpolarized electron beams whose energy is of the order of the molecular ionization potential (I). A phenomenological analysis of this possibility has been presented¹⁰ and quantitative estimates of the effects to be expected (an induced helicity between 10^{-3} and 10^{-5} in an initially unpolarized electron beam) have been made²⁵. These estimates show that observation of the helicity is not possible using available techniques, a result corroborated by the preliminary experiments sensitive to an induced helicity of order 10^{-2} which have not seen an effect¹¹.

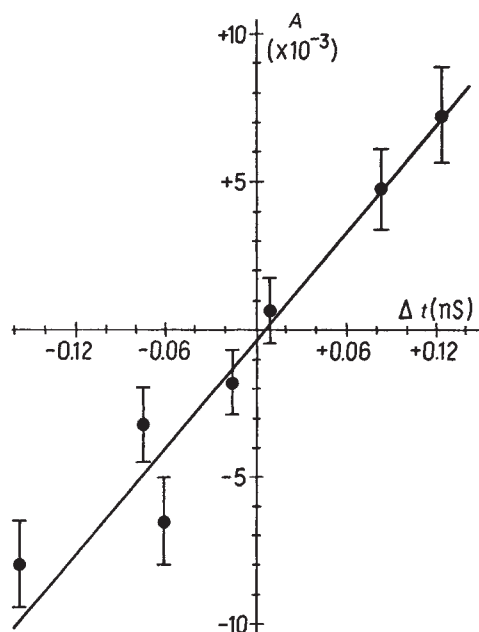


Fig. 3 The observed asymmetry in triplet Ps formation on DL cystine plotted against $\Delta\tau$, the observed time difference between the prompt peaks after helicity reversal. Values of r^+ and r^- based on $\sim 16 \times 10^6$ prompt time events and 10^6 delayed events were used to calculate A_{Ps} , according to equation (4). The uncertainties in A_{Ps} for a 12-h sequence were typically of order 10^{-3} based on Poisson (\sqrt{N}) statistics for prompt and delayed counts. The straight line is the linear least squares fit.

Table 1 The residual asymmetry, $A_{Ps}(0)$, and the χ^2 per degree of freedom obtained from the least squares fitting procedure

Substance	D	L	DL	
Cystine	$A_{Ps}(0) (\times 10^{-4})$	-10.8 (5.1)	-3.6 (5.0)	-4.2 (4.9)
	χ^2/N	4.8/5	7.4/7	6.2/7
Leucine	$A_{Ps}(0) (\times 10^{-4})$	-15.1 (7.3)	+4.0 (6.6)	-3.3 (3.2)
	χ^2/N	4.4/5	7.3/8	7.1/6
Tryptophan	$A_{Ps}(0) (\times 10^{-4})$	-2.7 (4.6)	-1.3 (5.5)	-10.9 (3.1)
	χ^2/N	0.7/3	3.9/4	7.0/7

In our experiment we employ a method that is much more sensitive to $h(\vec{r})$ than the radiolysis experiments. A beam of 200–400 eV positrons with a net helicity, $h(e^+)$, is directed into an amino acid target. After slowing down to ~ 10 eV, 80% of the positrons annihilate directly with an electron. The remaining 20% capture an electron to form positronium (Ps), the hydrogen-like bound state of the two particles. The Ps is formed in both the triplet (140 ns lifetime) and singlet (0.1 ns lifetime) spin states and the experiment is designed to detect only the triplet state (based on its long lifetime). Because of the existence of $h(\vec{r})$ in the molecule, the fraction of this state formed for a given isomer $f(L)$ or $f(D)$ depends on the sign and magnitude of $h(e^+)$ that is we have $f^+(L)$, $f^+(D)$ for $h(e^+) > 0$ and $f^-(L)$, $f^-(D)$ for $h(e^+) < 0$. As in radiolysis, $f^+(D) = f^+(L)$. The asymmetry A_{Ps} in the triplet Ps formation fraction on either reversal of $h(e^+)$ ($h(e^+) \rightarrow -h(e^+)$) or interchange of L and D isomers is:

$$A_{Ps} = \frac{f^+(L) - f^-(L)}{f^+(L) + f^-(L)} = \frac{f^+(L) - f^+(D)}{f^+(L) + f^+(D)} = |h(e^+)| H_{Ps}(Z) \quad (2)$$

Symmetric expressions for A_{Ps} based on interchange of $f^+(L) \rightarrow f^-(D)$ and so on may also be written. Here $H_{Ps}(Z)$ is directly analogous to $H_R(E, Z)$, but without the E dependence since Ps formation in a solid occurs in a narrow energy range below the molecular ionization potential. A detailed calculation of $H_{Ps}(Z)$ (ref. 3) shows that in our experimental conditions $H_{Ps}(Z)$ is expected to satisfy the inequality $10^{-6} < H_{Ps}(Z) < 10^{-5}$, for $Z = 6$, although in atypical cases values as large as $H_{Ps}(Z) \sim 10^{-2}$ have not been ruled out. As in the calculation of H_R , the major uncertainty in $H_{Ps}(Z)$ arises from uncertainty in the molecular wave functions.

An approximate general expression³ relating H_R to H_{Ps} may be written as

$$H_R(E, Z) = H_{Ps}(Z) \left(\frac{\eta'_R}{\eta_{Ps}} \right) \left(\frac{1}{2E_p \ln(2E_p)} \right) \quad (3)$$

where η_{Ps} is a molecular asymmetry factor for $H_{Ps}(Z)$, analogous to η'_R for radiolysis. The value of η_{Ps} has been calculated for the simplest optically active molecule for which the most complete wavefunctions are available, 15° twisted ethylene³, with the result $\eta_{Ps} \sim 10^{-2}$. While η'_R has not been so calculated, it is estimated to be of the same order of magnitude as η_{Ps} (although the relative signs are not yet determined). Thus we find that $|H_R| \approx 10^{-3} |H_{Ps}(Z)|$. Our goal is to measure A_{Ps} and $h(e^+)$ and thus determine or set upper limits on $H_{Ps}(Z)$ so that the quantities of fundamental chemical and biological interest, $h(\vec{r})$ and $H_R(E, Z)$, may be estimated.

Experiment

The apparatus is designed to measure the amount of triplet Ps formed when an amino acid powder target is bombarded with a collimated beam of positrons whose energy and helicity can be varied. The asymmetry in triplet Ps production (A_{Ps}) under reversal of either positron helicity (+, -) or target chirality (L, D) is then determined. The apparatus used to produce the beam is sketched in Fig. 1 and discussed in detail in ref. 12.

Figure 1 shows the positrons focused onto the surface of a channel electron multiplier (CEM) coated with the optically active material under investigation, where their impact is detected through emission of secondary electrons (see Fig. 2). Detection of one or more of the annihilation γ s in Pilot B plastic scintillator detectors (Fig. 1) provides the 'stop' signal following

the CEM 'start' signal which allows the lifetime of each positron event to be measured directly. The lifetime spectrum so obtained consists of an ~ 1 ns wide 'prompt peak' of directly annihilating positrons together with Ps which annihilates within the amino acid, the 140 ns exponential component of free triplet Ps, and a uniform background from uncorrelated events. To correct for variations in beam intensity, a ratio of counts from triplet events (background subtracted), occurring in a 400 ns wide time window starting at 75 ns after the prompt peak ($t = 0$), to counts in the prompt peak is calculated. Defining r^+ to be this ratio for incident positron helicity positive (r^- for $h(e^+) < 0$) A_{Ps} (equation (2)) is given by

$$A_{Ps} = (r^+ - r^-)/(r^+ + r^-). \quad (4)$$

Asymmetry measurements were made by reversing $h(e^+)$ every 330 s during a 12-h period. The cumulative lifetime spectrum for each value of $h(e^+)$ was stored in memory halves of a multichannel analyser. The large number of helicity reversals per run reduced the effect of random and secular time shifts in the $t = 0$ position of the prompt peak to < 0.01 ns. Asymmetries were measured in this manner for samples of D, L, and DL isomers of tryptophan, cystine and leucine (supplied by Sigma Chemical Co.).

Variations in the measured asymmetries for preliminary runs were found to be greatly in excess of statistical fluctuations. Experiments showed that the Ps formation fraction could vary by as much as 20% over the surface of the CEM cone, depending on how far from the channel entrance the positron strikes the cone (see Fig. 2). As a result, changes in the size, shape, and position of the positron beam under helicity reversal could produce false asymmetries as large as 1%. Such systematic effects could be separated from any true isomeric asymmetry by noting that the time-of-flight of the secondary electrons ejected from the cone (and hence the observed time difference, $\Delta\tau$, in the prompt peak after helicity reversal), has also been shown to depend on how far from the channel entrance the beam strikes the CEM. Thus the observed asymmetries A_{Ps} with their correlated values of $\Delta\tau$ could be fit to the equation $A_{Ps} = m\Delta\tau + A_{Ps}(0)$ where m and $A_{Ps}(0)$ are the fitted parameters; and $A_{Ps}(0)$, the residual asymmetry at $\Delta\tau = 0$, is the quantity of interest. An example of the fit is shown in Fig. 3 and the results for the isomers of cystine, tryptophan and leucine are shown in Table 1.

The uncertainties in the results are statistical uncertainties for the fitted data. As evidence by the χ^2 test the linear hypothesis is statistically compatible with the data for the D, L and DL samples of cystine and tryptophan. However, using the original statistically assigned uncertainty, the data of D and L leucine yielded χ^2/N in excess of 2. In view of the still incompletely understood nature of the systematic effects discussed above, we increased the uncertainty on the individual data points to make $\chi^2/N \approx 1$. The uncertainty in $A_{Ps}(0)$ and χ^2/N (leucine) in Table 1 reflect this adjustment.

The measured values of $A_{Ps}(0)$ (Table 1) show no statistically significant difference between the D and L isomers of cystine and tryptophan at the 7×10^{-4} level but the data do indicate the possibility of an effect at the 2σ level in leucine. In view of this possible effect additional data on leucine were obtained in which an attempt was made to maintain $\Delta\tau$ at a sufficiently low level ($\Delta\tau < (0.02 \pm 0.02)$ ns) so that the values of A_{Ps} from several independent runs could simply be averaged without relying on the fitting procedure described above. This was accomplished by adjusting the beam deflection electrodes before each run. The weighted averages and values of χ^2 per degree of freedom obtained using this procedure were $A_{Ps}(D) = -(30.0 \pm 4.9) \times 10^{-4}$, $A_{Ps}(L) = +(1.3 \pm 4.4) \times 10^{-4}$, $\chi^2(D)/N = 5.6/6$ and $\chi^2(L)/N = 11/7$.

The above result seems to indicate the detection of an L/D asymmetry in triplet Ps formation in leucine of $(31 \pm 7) \times 10^{-4}$. However, in view of the large systematic effect discussed previously (values of A_{Ps} of up to -60×10^{-4} were observed in leucine for $\Delta\tau \sim 0.1$ ns) and in view of the fact that $A_{Ps} \sim$

30×10^{-4} is a much larger effect than predicted by theory³, we feel that this result is still preliminary, and while suggestive of an effect, it is not definitive. A newly designed experiment is under construction in which the systematic effects related to beam parameters and detector geometry should be eliminated. We conclude that we have established A_{Ps} to be $< 7 \times 10^{-4}$ in cystine and tryptophan, but that there may be an effect in leucine. We note that previous work by Bonner *et al.*⁷ did show asymmetric L/D radiolysis by polarized electrons in leucine but that this effect was not corroborated by Hodge *et al.*⁸.

To relate A_{Ps} to $H_{Ps}(Z)$ (equation (2)) it is necessary to obtain the positron helicity ($h(e^+) = \langle \hat{s}_i \rangle \cdot \langle \hat{p}_i \rangle$) not for the incident positron beam (recall $h_0(e^+) = 0.21$), but for the beam after it has slowed down in the target to Ps formation energies (≤ 10 eV). This final helicity ($h_f(e^+)$) is not directly observable but it can be estimated theoretically. Many experiments^{12,13} have shown that, in agreement with theoretical predictions¹⁴, the magnitude and direction of $\langle \hat{s} \rangle$ for an ensemble of positrons is essentially unchanged when the positrons slow down to Ps formation energies from energies far in excess of the initial 400 eV energy used in this experiment. Although $\langle \hat{s}_i \rangle$ is constant, the magnitude of $\langle \hat{p}_i \rangle$ ($|\langle \hat{p}_i \rangle|$) does decrease as the beam slows down and this increased beam divergence can be calculated for positrons of the energies we use incident on metal surfaces^{15,16}. For the case of $|\langle \hat{p}_i \rangle|_{\text{initial}} = 1$, the beam divergence after n collisions is given by $|\langle \hat{p}_i \rangle| = \cos \theta = [\cos \theta_1 \cos \theta_2 \cdots \cos \theta_n]$. The theoretical results are generally in good qualitative agreement with experiment^{17,18}.

The calculation of $\cos \bar{\theta}$ using the formulas of refs 17, 18 may be generalized to the case of the amorphous insulator alumina (Al_2O_3) based on calculations of specific energy loss (dE/dx) and mean free path between collisions (λ)¹⁹. The final extrapolation to the amino acids used in our experiment is made based on the assumption that dE/dx and λ may be scaled from one substance to another because the probability of a positron-atom interaction is proportional to $N\sigma$ where N is the number of electrons/atom with which the positron can interact (essentially valence electrons) and σ is the positron-atomic electron interaction cross-section (taken as constant in all amorphous insulators).

The results of the calculation yield a final value of $\cos \bar{\theta} = (0.4 \pm 0.2)$ or $h_f(e^+) = h_0(e^+) |\langle \hat{p}_i \rangle| \approx 0.2 \times 0.4 = (0.08 \pm 0.04)$. The error assignment results from systematic uncertainties in the correct number of valence electrons to use in a given amino acid and the nature of various approximations of the scattering cross-sections used in ref. 19.

Conclusion

Our experiment aims to determine $H_{Ps}(Z)$, or set limits on it, so that the quantity of interest relating to the origin of optical activity $H_R(E, Z)$ may be determined (equation (3)), and so that the newly identified property of chiral molecules, the helicity density $h(\vec{r})$, may be investigated. From equation (2) and the value $h_f(e^+) \approx 0.08 \pm 0.04$ we have $H_{Ps}(Z) \leq (A_{Ps}/h(e^+)) = (7 \times 10^{-4}/8 \times 10^{-2}) \approx 10^{-2}$ for cystine and tryptophan. The possible value of $H_{Ps}(Z)$ for leucine where an effect of $A_{Ps} = (31 \pm 7) \times 10^{-4}$ may have been observed is $H_{Ps}(Z) \approx (31 \times 10^{-4}/8 \times 10^{-2}) \sim (4 \pm 2) \times 10^{-2}$.

Comparing the above results with previous measurements²⁰⁻²³ using positrons we note that, in all cases, positrons from a radioactive source slowed to positronium formation energies directly in the amino acid, implying⁹ $h_f(e^+) < 10^{-2}$. Three experiments²⁰⁻²² gave null values of A_{Ps} at the 10^{-2} level, which if combined with the estimated $h_f(e^+)$, yield $H_{Ps}(Z) < 10$. The positive results of ref. 23 imply $H_{Ps}(Z) \approx 100$. Thus the results of the present experiment, implying $H_{Ps}(Z) \leq 10^{-2}$ in three cases and $H_{Ps}(Z) = 4 \times 10^{-2}$ in the fourth, although larger than the theoretical predictions of ref. 3 ($H_{Ps}(Z) < 10^{-5}$), are the first to set limits on $H_{Ps}(Z)$ which have any reasonable physical meaning, that is $H_{Ps}(Z) < 1$. Finally, using equation (3), our limits on $H_{Ps}(Z)$ enable us to set the upper limit

$H_R(E, Z) < 10^{-7}$. This represents an improvement of 10^4 over the limits of 10^{-3} set by direct radiolysis experiments.

Plans for future experiments involve changes to reduce the instrumental asymmetries and to increase the beam rate by an order of magnitude. In addition, we are now able to increase beam polarization up to 0.7 (J.V.H and P.W.Z in preparation). These and other changes should enable us to improve our limits on H_{Ps} by a further factor of ~ 100 , sufficient to observe an effect if $H_{Ps}(Z) \sim 10^{-4}$, a value within theoretical

bounds. Finally, the predicted³ increase in asymmetry with Z^2 will be tested using amino acids with heavy atoms ($Z > 30$) at the chromophore. Observation of the asymmetry in such a molecule should be within reach of the next generation experiment.

We thank Professors G. W. Ford, R. A. Hegstrom, G. Karl, R. R. Lewis, and J. Walker for helpful discussions and R. H. Sands for major equipment loans. This work is supported by NASA and by the NSF.

Received 30 December 1981; accepted 7 April 1982.

1. Kizel, V. A. *Soviet Phys. Usp.* **23**, 277–295 (1980).
2. Norden, B., *J. molec. Evolut.* **11**, 313–332 (1978).
3. Hegstrom, R. A. *Nature* **297**, 643–647 (1982).
4. Norden, B. *Nature* **266**, 567–568 (1977).
5. Angel, J. R. P. & Illing, R. *Nature* **238**, 389–390 (1972).
6. Keszthelyi, L. *Origins of Life* **8**, 299–340 (1977).
7. Bonner, W. A., Van Dort, M. A. & Yearian, M. A. *Nature* **258**, 419–421 (1975).
8. Hodge, L. A., Dunning, F. B. & Walters, G. W. *Nature* **280**, 250–252 (1979).
9. Rich, A. *Nature* **264**, 482 (1976).
10. Farago, P. *J. Phys. B* **13**, L567–569 (1980); **14**, L743–748 (1981).
11. Beerlage, M. J. M., Farago, P. S. & Van der Wiel, M. J. *J. Phys. B* **14**, 3245–3253 (1981).
12. Gerber, G., Newman, D., Rich, A. & Sweetman, E. *Phys. Rev. D* **15**, 1189–1193 (1977).

13. Zitzewitz, P. W., Van House, J. C., Rich, A. & Gidley, D. W. *Phys. Rev. Lett.* **43**, 1281–1284 (1979).
14. Bouchiat, C. & Levy-Leblond, L. M. *Nuovo Cim.* **33**, 193–200 (1964).
15. Oliva, J. *Phys. Rev. B* **21**, 4909–4924 (1980).
16. Nieminen, R. M. & Oliva, J. *Phys. Rev. B* **22**, 2226–2247 (1980).
17. Lanteri, H., Bindiet, R. & Rostaing, P. *Thin Solid Films* **67**, 293–299 (1980).
18. Hrach, R. *Thin Solid Films* **15**, 65–69 (1973).
19. Ritchie, R. H., Garber, F. W., Nakai, M. Y. & Birkhoff, R. D. *Adv. Radiat. Biol.* **3** (1969).
20. Dezsi, I., Horvath, D. & Kajcos, Z. S. *Chem. Phys. Lett.* **24**, 514–515 (1974).
21. Brandt, W. & Chiba, T. *Phys. Lett.* **57A**, 395–396 (1977).
22. Jean, Y. C. & Ache, H. J. *J. chem. Phys.* **81**, 1157–1162 (1977).
23. Garay, A. S., Keszthelyi, L., Demeter, I. & Hrascko, P. *Nature* **250**, 332–333 (1974); *Chem. Phys. Lett.* **23**, 549–552 (1973).
24. Gidley, D. W., Rich, A., Van House, J. C. & Zitzewitz, P. W. *Origins of Life* **11**, 31–36 (1981); in *Origin of Life*, (ed. Wohlman, Y.) 379–384 (Reidel, Boston, 1981).
25. Rich, A., Van House, J. & Hegstrom, R. A. *Phys. Rev. Lett.* **48**, 1341–1344 (1982).

β Decay and the origins of biological chirality: theoretical results

Roger A. Hegstrom

Department of Chemistry, Wake Forest University, Winston-Salem, North Carolina 27109, USA

A dynamical mechanism is found whereby a dissymmetric molecule and its mirror image are ionized at different rates by longitudinally polarized electrons such as produced by nuclear β decay. An enhancement is predicted for molecules containing heavy atoms. Order-of-magnitude estimates indicate that the asymmetric effect of this mechanism may be detectable by current experiments on positronium formation.

THE postulated existence of a causal relationship between the parity nonconserving aspect of the weak interaction and the observed dissymmetry of the molecules present in living organisms^{1–3} seems reasonable as the weak interaction is universal and always acts in the same chiral sense. Hence if an effective mechanism exists involving the weak interaction in molecular evolution, this inherent universal chirality in nature could have influenced the selection of exclusively D sugars for RNA and DNA and L amino acids for proteins.

Two candidates for such a mechanism have been proposed, each of which involves a different aspect of the weak interaction. One produces an energy difference between a chiral molecule and its mirror image⁴, but the calculated difference⁵ seems too small to have been effective in molecular evolution. The other, which seems the most popular theory at present, postulates the asymmetric radiolysis of racemic mixtures of prebiotic chiral molecules by the longitudinally polarized electrons produced in nuclear β decay⁶. A precise test of some aspects of this mechanism is the object of new experiments to measure an asymmetry in the rate of triplet positronium (Ps) formation in chiral molecules discussed in the accompanying article⁷ (where references to previous work may be found).

The present article gives a theoretical basis for, and estimates the magnitudes of, the cross-section asymmetries for both Ps formation and radiolysis. The relevance of the results to the question of the origin of chirality in living organisms is discussed extensively in the preceding article⁷.

Ps formation in optically active molecules

The treatment of the asymmetry in the cross-section for positronium formation given here and that for radiolysis which follows are based on nonrelativistic scattering theory. The notation of Taylor⁷ is followed except that atomic units are used here ($\hbar/2\pi = e = m_e = 1$, where \hbar is Planck's constant, e the electron charge, and m_e the electron mass).

Consider a positron with momentum \vec{p} and helicity $\lambda = \vec{\sigma} \cdot \hat{p} = \pm 1$, where $\hat{p} = \vec{p}/p$ and $p = |\vec{p}|$, incident on an optically active molecule, the nuclei of which are taken to be fixed in the laboratory frame of reference (Fig. 1). This initial channel is labelled α , and α' labels the final channel which consists of the ionized molecule and a Ps atom with momentum \vec{P}' . Spin is quantized along \vec{p} and hence the spin projection quantum number of the positron is related simply to the helicity by $m_\lambda = \frac{1}{2}\lambda$. The cross-section depends on the helicity λ , the chirality of the target molecule (L or D), and on the spin state S of the Ps, and is given by

$$\sigma_S^\lambda(L) = (2\pi)^4 \frac{P'}{p} \int |t_S^\lambda(L)|_{Av}^2 d\Omega' \quad (1)$$

(with a corresponding expression for the D isomer) where $P' = |\vec{P}'|$, where $d\Omega'$ denotes an integration over the solid angles corresponding to directions of \vec{P}' , and where Av denotes an average over all orientations of the molecule (random orientations are assumed). The quantity t_S^λ , which is related to the on-shell T-matrix, is defined below.

In a notation consistent with that of the preceding paper⁷, the asymmetry in the cross-section is defined as

$$H_{Ps}(L) \equiv \frac{\sigma_S^+(L) - \sigma_S^-(L)}{\sigma_S^+(L) + \sigma_S^-(L)} = \frac{\sigma_S^+(L) - \sigma_S^+(D)}{\sigma_S^+(L) + \sigma_S^+(D)} \quad (2)$$

(with a corresponding equation for the D isomer) where $\sigma_S^+(L)$ and $\sigma_S^-(L)$ are obtained from equation (1) with $\lambda = +1$ and $\lambda = -1$ respectively. The second equation in equation (2) is a consequence of parity conservation for the electromagnetic interaction [equations (6, 7)], from which the general relationship $\sigma_S^\lambda(L) = \sigma_S^{-\lambda}(D)$ follows. For the case of a positron beam of helicity $h(e^+)$ and with $h \equiv |h(e^+)| \leq 1$, it can be shown that, for a given L or D isomer (from now on the isomer is not denoted explicitly), the asymmetry in the cross-section obtained